

Oscillations of metal-plate impedance and character of electron reflection

I. F. Voloshin, N. A. Podlevskikh, V. G. Skobov, L. M. Fisher, and A. S. Chernov

V. I. Lenin All-Union Electrotechnical Institute

(Submitted 25 May 1982)

Zh. Eksp. Teor. Fiz. **83**, 1955–1970 (November 1982)

The surface impedance of a metallic plate as a function of a magnetic field perpendicular to the plate is investigated theoretically and experimentally. The integro-differential equation for the rf field distribution in the plate is solved under the assumption that electron reflection from the surface can be described by an arbitrary Fuchs specular coefficient p . A solution is obtained for magnetic field values greatly exceeding the dopplerson threshold field. The plate impedance is calculated on the basis of the obtained field distribution. The influence of specularly reflected electrons on the shape of the impedance oscillations is studied. It is shown that analysis of the shapes of the dopplerson oscillations and of the Gantmakher-Kaner oscillations can yield the value of p for resonant carriers. A method is developed for the analysis of the shape of the experimentally recorded oscillations. Tungsten-plate-impedance measurements needed to determine the specularity coefficient of resonant electrons and their mean free paths are performed. The values of the specularity coefficients are found. The behavior of p when the magnetic field deviates from normal to the surface is studied experimentally.

PACS numbers: 75.70.Dp

A considerable number of studies of the character of electron reflection from a metal surface have been recently reported. Experimental data indicating that the electron reflection is not completely diffuse were obtained. Tsoi¹ proposed a method for measuring the specularity parameter p by focusing electron beams in a transverse magnetic field. Another method of determining p is based on measurement of the anharmonicity of the Sondheimer oscillations.² We deemed it attracting to use for the same purpose the oscillations of the rf impedance of a plate in a perpendicular magnetic field H . The difficulty lay in the extreme difficulty of calculating the plate impedance for nonspecular electron reflection. A rigorous theory of radiowave propagation in a metal for the case $p = 0$ was developed in Ref. 3 and is valid in a wide range of magnetic field. In the present paper (§1) we derive general expressions for the field distribution and the plate impedance in strong magnetic fields $(H/H_L)^3 \gg 1$ (H_L is the dopplerson threshold field) at arbitrary values of the parameter p . The impedance behavior in strong field is determined mainly by the resonant carriers and is independent of the details of the Fermi surface. This circumstance, as well as the simplicity of the expressions obtained, permits a quantitative comparison of the theory with experiment. The final results of the theory are given for symmetric and antisymmetric excitations of the plate. Analysis of the waveform of the impedance oscillations is the subject of §2. The waveform distortion in both dopplerson oscillations and Ganmakher-Kanner oscillations (GKO) is analyzed in detail. The GKO are analyzed using as an example a metal with a corrugated-cylinder Fermi surface. Formulas are obtained for the specularity coefficient in terms of experimentally observable quantities. The transition from impedance to transverse magnetoresistance is demonstrated at the end of the section for linear polarization and for symmetric excitation. In §3 are described the measurement technique and the procedure for the analysis of the impedance-oscillation waveform. The

use of a modulation procedure made possible a Fourier analysis of the oscillations directly in the course of the measurements. Separation and recording of the first and then the second harmonic of the signal as functions of the magnetic field have made it possible to simplify considerably and increase the accuracy of the determined degree of anharmonicity of the oscillations.

The results of the experimental study of the impedance and of the oscillation waveform are present in §4 for tungsten and cadmium plates. The measured anharmonicity of the oscillations when the magnetic field is inclined away from the normal to the surface are also cited there. In §5 we obtain the specularity coefficient p from the results of measurements of different samples and from the equations of the theory developed. With tungsten and cadmium as examples, we analyze the advantages and difficulties of the proposed method of determining the coefficient p for a resonant group of carriers in actual metals. The cause of the decrease of the effective value of p when the magnetic field is inclined are discussed. It is shown at the end of the section that the dependence of the amplitude of the d^2R/dH^2 oscillations on p is complicated and is not the same in different magnetic fields.

§1. FIELD DISTRIBUTION AND PLATE IMPEDANCE

1. The distribution of a field $\mathcal{E}_\alpha(z)$ that is homogeneous in the xy plane is described by Maxwell's equations

$$\frac{d^2 \mathcal{E}_\alpha}{dz^2} = -\frac{4\pi i \omega}{c^2} j_\alpha(z) \quad (\alpha = x, y), \quad (1)$$

where ω is the electromagnetic-field frequency and j_α is the current density in the metal. In an infinite metal the current is

$$j_\alpha(z) = \int_{-\infty}^{\infty} \sigma_{\alpha\beta}(z-z') \mathcal{E}_\beta(z') dz', \quad (2)$$

where $\sigma_{\alpha\beta}(z)$ is the metal nonlocal-conductivity tensor. We

shall omit hereafter the tensor indices and introduce the notation

$$T(z) = (4\pi i \omega / c^2) \sigma(z). \quad (3)$$

For a metal plate bounded by two surfaces $z = 0$ and $z = d$, the expression for the current takes the form

$$\begin{aligned} \frac{4\pi i \omega}{c^2} j(z) = & \int_0^d \left[\sum_{k=-\infty}^{\infty} T(z-z'-2kd) p^{2k} \right. \\ & \left. + \sum_{k=-\infty}^{\infty} T(z+z'-2kd) p^{2k-1} \right] \mathcal{E}(z') dz', \quad (4) \end{aligned}$$

where p is the Fuchs phenomenological parameter that describes electron reflection from a metal surface. It is assumed here that, except for the plate surfaces, the electron trajectory has no points at which the electron longitudinal velocity v_z reverses sign. Each of the terms in the sums of (4) is the contribution of electrons that had experienced a number of collisions, from each of the surfaces, as they moved from point z' to point z . To simplify (4), we made use of the fact that $\sigma(z)$ is an even function.

Obviously, a general solution of Eqs. (1) and (4) can be represented as a linear superposition of two solutions, one symmetric and the other asymmetric with respect to the midplane of the plate $z = d/2$. Both solutions are found in similar manner. We solve therefore the problem for antisymmetric excitation, and present only the final result for the symmetric one.

Using the fact that $\mathcal{E}_a(z') = -\mathcal{E}_a(d-z')$, we change the variable in the integral that contains the second sum in (4). The equation for the field distribution in the plate takes as a result the form

$$\frac{d^2 \mathcal{E}_a}{dz^2} + \int_0^d \sum_{n=-\infty}^{\infty} (-p)^{|n|} T(z-z'-nd) \mathcal{E}_a(z') dz' = 0. \quad (5)$$

2. Following the basic idea of Ref. 3, we attempt to represent $\mathcal{E}_a(z)$ as a difference of two expressions, each containing only field components propagating in one definite direction of the z axis. We rewrite first Eq. (5), defined on the segment $[0, d]$, in the form

$$\frac{d^2 \tilde{\mathcal{E}}}{dz^2} + \int_{-\infty}^{\infty} T(z-z') \tilde{\mathcal{E}}(z') dz' = 0, \quad 0 \leq z \leq d, \quad (6)$$

where

$$\begin{aligned} \tilde{\mathcal{E}}(z) = & (-p)^{|n|} \mathcal{E}_a(z-nd), \quad nd < z < (n+1)d, \\ n = & 0, \pm 1, \pm 2, \dots \quad (7) \end{aligned}$$

We introduce the function $f(z)$ defined on the right-hand half of the straight line by the equation

$$\frac{d^2 f}{dz^2} + \int_{-\infty}^{\infty} T(z-z') f(z') dz' = 0, \quad 0 \leq z < \infty, \quad (8)$$

and on the left side by some external condition. It is easy to verify that the combination

$$e_a(z) = e_p(z) - e_p(d-z), \quad (9)$$

where

$$e_p(z) = \sum_{k=0}^{\infty} (-p)^k f(z+kd), \quad (10)$$

satisfies on the segment $[0, d]$ the equation

$$\frac{d^2 e_a}{dz^2} + \int_{-\infty}^{\infty} T(z-z') e_a(z') dz' = 0, \quad 0 \leq z \leq d. \quad (11)$$

Equation (11) coincides with (6) if the function $f(z)$ is additional defined on the left-hand line so that the function $e_a(z)$ has the property (7). Using the resultant condition

$$f(z) = pf(-z) + (1-p^2) \sum_{k=0}^{\infty} (-p)^k f((k+1)d-z), \quad z < 0 \quad (12)$$

and changing the variable in some of the integrals, we rewrite (8) in the form

$$\begin{aligned} \frac{d^2 f}{dz^2} + \int_0^{\infty} T(z-z') f(z') dz' + p \int_0^{\infty} T(z+z') f(z') dz' \\ = - (1-p^2) \int_0^{\infty} T(z+z') \sum_{k=0}^{\infty} (-p)^k f((k+1)d+z') dz', \quad z \geq 0. \quad (13) \end{aligned}$$

After changing the integration variables, Eq. (13) contains only the values of the function $f(z)$ on the right-hand half-line, so that it can be arbitrarily redefined on the left-hand half, say, $f(z < 0) = 0$.

Thus, relations (9)–(10) together with the solution of (13) determine the field distribution in an asymmetrically excited plate of thickness d .

As $d \rightarrow \infty$ the right-hand side of (13) tends to zero and the equation coincides with that for the field distribution in a semi-infinite metal⁴ (in this case the second term of (9) is zero and only the term with $k = 0$ remains in the sum (10)). In the case of diffuse reflection ($p = 0$ but d is finite) Eq. (13) coincides with the basic Eq. (26) of Ref. 3, and the sum (10) again consists only of one term. Finally, at $p = 1$ the right-hand side of (13) vanishes, the solution is solved by Fourier transformation, and the sum (10) is easily calculated. The resultant expression coincides with the result of Ref. 5.

The equations for the field distribution under symmetric excitation are

$$e_s(z) = e_p^s(z) + e_p^s(d-z), \quad (14)$$

$$e_p^s(z) = \sum_{k=0}^{\infty} p^k f_s(z+kd), \quad (15)$$

$$\begin{aligned} \frac{d^2 f_s}{dz^2} + \int_0^{\infty} f(z') dz' [T(z-z') + pT(z+z')] \\ = (1-p^2) \int_0^{\infty} T(z+z') \sum_{k=0}^{\infty} p^k f((k+1)d+z') dz', \quad z \geq 0. \quad (16) \end{aligned}$$

3. Consider a metal plate placed perpendicular to a magnetic field \mathbf{H} under conditions when the magnitude of \mathbf{H} and the frequency ω of the exciting electromagnetic field satisfy the inequalities $\omega \ll \nu \ll \omega_c$, where ω_c is the cyclotron frequency of the carriers and ν is their collision frequency. Let the symmetry axis of the Fermi surface of the electrons be likewise directed normal to the plate, and let the electron

displacement during the cyclotron period, as a function of the longitudinal momentum, have one maximum u . If, however, other types of carrier are present, their displacement is assumed to be small compared with u and their contribution to conductivity will be described in the local approximation.

In the situation described the system (1) and (4) breaks up into two equations for the circular polarizations $\mathcal{E}_+ = \mathcal{E}_x \pm i\mathcal{E}_y$. We obtain below equations for the "minus" circular polarization, in which the field rotates in the same direction as the electrons, and will cite the final result for the "plus" polarization. Next, we use the dimensionless coordinate $\xi = 2\pi z/u$ and the dimensionless wave vector $q = ku/2\pi$, where k is the wave vector. In these variables, the Fourier component of the nonlocal conductivity $\sigma(q)$ has in the complex q plane two branch points $q = \pm(-1 + i\gamma)$, the cuts from which we draw respectively to $\mp\infty$; here $\gamma = v/\omega_c$.

The dispersion equation that characterizes the eigenmodes in the metal will be written in the form

$$D(q) = 0, \quad (17)$$

where

$$D(q) = q^2 - K(q), \quad K(q) = \xi H \sigma(q) / nec, \quad \xi = \omega n e u^2 / \pi c H, \quad (18)$$

and n is the electron density. In strong magnetic fields, where $\xi \ll 1$, one of the roots of (17), q_1 , is small, and the second, doppleron root, is close to -1 . The doppleron threshold H_1 , i.e., the lower limit of the magnetic field region, where the root q_2 remains almost real, corresponds to $\xi = \xi_L$, where ξ_L is a numerical constant of the order of unity and depends on the model. Using this constant, we can represent ξ in the form $\xi = \xi_L (H_L/H)^3$.

4. Using the dimensionless variables, we rewrite (13) in the form

$$\frac{d^2 f}{d\xi^2} + \int_0^\infty K(\xi - \xi') f(\xi') d\xi' = - \int_0^\infty K(\xi + \xi') [p e_p(\xi') + e_p(\xi' + L)] d\xi', \quad (19)$$

where $L = 2\pi d/u$. To solve (19) in the strong-field region $\xi \ll 1$ we need the solution of an equation similar to (19) but with a zero right-hand side. It comprises the field distribution in semi-infinite metal at $p = 0$, and takes according to Eqs. (3), (4), (19), and (21) of Ref. 3 the form

$$e_0(\xi) = \frac{1}{2\pi i} \int_{-\infty}^\infty \frac{(q+q_1) e^{iq\xi}}{D(q)} dq = e^{iq_1 \xi} + b_0 e^{iq_2 \xi} + \frac{1}{2\pi i} \int_{C_-} \frac{q e^{iq\xi}}{D(q)} dq, \quad (20)$$

where C_- is the contour drawn counterclockwise around the left-hand cut of the q plane, and

$$b_0 = - \left(\frac{dD}{dq} \Big|_{q=q_2} \right)^{-1}. \quad (21)$$

The field e_0 consists of three components: long-wave, dop-

pleron, and Gantmakher-Kaner component (GKC). The wave vector corresponding to the asymptote of the GKC at $\xi \gg 1$ is equal to -1 . For all models but one, the GKC amplitude is proportional to ξ , and $b_0 = \partial(\xi)$ for a Fermi surface in the form of a parabolic lens, $b_0 = -\xi/2$, and the GKC is identically equal to zero.

To solve (19) we use the fact that the short-wave-component amplitudes in strong fields ($\xi \ll 1$) have small amplitudes. The field distribution in the plate consists in practice of the same components, but with different coefficients. The short-wave component amplitudes, however, remain small. It suffices therefore to retain only the long-wave component in the integral in the right-hand side of (19). The point is that the function K in this integral depends on the sum $\xi + \xi'$ and the oscillations of the various terms in the integrand are of the same order. On the other hand, in the integral of the left-hand side of (19) no such simplification is possible. Here the term proportional to the long-wave component oscillates rapidly, as before, and the oscillations of the short-wave components and of the conductivity $K(\xi - \xi')$ cancel out in that part of the integral where $\xi' < \xi$. As a result, the contribution of all the components may turn out to be of the same order.

We seek a solution of (19) in the form

$$f(\xi) = (1 + p e^{iq_1 L}) e^{iq_1 \xi} + U(\xi), \quad (22)$$

where $U(\xi)$ constitutes the short-wave components. The right-hand side of (19) takes then the form

$$-(p + e^{iq_1 L}) \int_0^\infty K(\xi + \xi') e^{iq_1 \xi'} d\xi'. \quad (23)$$

We use now some results of Ref. 3. Equation (26) of that reference takes in strong field the form (19) with a right-hand side given by

$$-e^{iq_1 L} \int_0^\infty K(\xi + \xi') e^{iq_1 \xi'} d\xi'.$$

The solution of this equation, which satisfies the unity boundary condition, can be transformed for strong fields [using (46) and (60) of Ref. 3] into

$$e_0(\xi) = \frac{e^{iq_1 L}}{2\pi i} \int_{-\infty}^\infty \frac{(q - q_1) e^{iq\xi}}{D(q)} dq,$$

where the first term is the solution of the homogeneous equation and the second is a particular solution of the inhomogeneous one. The total solution of (19) with right-hand side (23) can therefore be written in the form

$$f(\xi) = A e_0(\xi) - (p + e^{iq_1 L}) \frac{1}{2\pi i} \int_{-\infty}^\infty \frac{(q - q_1) e^{iq\xi}}{D(q)} dq. \quad (24)$$

Calculating the factor of $\exp(iq_1 \xi)$ in this expression [see (20)] and comparing it with the factor of $\exp(iq_1 \xi)$ in (22), we obtain $A = 1 + p \exp(iq_1 L)$. We can now write the solution of (19):

$$f(\xi) = \frac{1}{2\pi i} \int_{-\infty}^\infty dq \frac{e^{iq\xi}}{D(q)} \{ q(1-p)(1 - e^{iq_1 L}) + q_1(1+p)(1 + e^{iq_1 L}) \}. \quad (25)$$

Substituting it in (10) and (9) and calculating the sums of the series, we obtain ultimately an expression for the magnetic-field distribution in the plate; this expression is valid in strong magnetic fields ($\xi \ll 1$),

$$e_a(\xi) = \frac{1}{2\pi i} \int_{-\infty}^{\infty} \frac{dq}{D(q)} \frac{e^{iq\xi} - e^{iq(L-\xi)}}{1 + pe^{iqL}} \times \{q(1-p)(1 - e^{iqL}) + q_1(1+p)(1 + e^{iqL})\}. \quad (26)$$

5. We calculate now the plate impedance

$$Z = (8\pi q_0/c) (ie_a(0)/e_a'(0)), \quad (27)$$

where $q_0 = \omega u/2\pi c$, and the prime denotes differentiation with respect to ξ . Substituting (26) in (27), we represent the expression for Z in the form

$$Z = [1 + (1+p)\alpha\delta] [Z_p^{-1} + a(1-p)\alpha\delta]^{-1}, \quad (28)$$

where

$$Z_p^{-1} = a[q_1 t_1^{-1} - i(e_0' - iq_1)(1-p)], \quad a = (c^2/4\omega u), \quad (29)$$

$$\alpha = (1-p) - (1+p)q_1 t_1^{-1}, \quad (30)$$

$$t_1 = [1 - \exp(iq_1 L)] [1 + \exp(iq_1 L)]^{-1}, \quad (31)$$

and

$$\delta = -\frac{b_0 e^{iq_2 L}}{1 + pe^{iq_2 L}} - \frac{1}{2\pi i} \int_{c_-} \frac{q dq}{D(q)} \frac{e^{iqL}}{1 + pe^{iqL}} \quad (32)$$

contains the oscillations with short period in terms of the magnetic field. To derive (28)–(32) we used Eq. (20) as well as the inequality $\xi \ll 1$. In addition, we took into account the inequality $L \gg 1$ and its corollaries. The last inequality is a necessary condition for observing oscillations in experiment. Finally, with the aid of inequality $\xi \ll 1$ we can write the expression (28) for the impedance in the form of a sum of parts that vary rapidly and slowly with the magnetic field:

$$Z = Z_p \{1 - aZ_p \alpha^2 \delta / [1 + aZ_p \alpha (1-p)\delta]\}. \quad (33)$$

We emphasize that in the derivation of (33) we did not use the smallness of the rapidly oscillating part. An expression for the smooth part of the impedance at arbitrary p , similar to (29), can be derived first in Ref. 6 in the case of small oscillations for a particular model of the "corrugated cylinder" type.

For the paraboloidal model, the result (29)–(33) coincides with the result that follows from (29) of Ref. 7. For $p = 1$ and for a Fermi surface of the corrugated cylinder type, we obtain the expressions of Ref. 8. If the oscillations constitute a small fraction of the impedance, we can discard the second term of the dominator in (33). In this case, at $p = 0$ and $|q_1| \ll 1$, Eqs. (29)–(33) go over into expressions (61) and (62) of Ref. 3.

To obtain expressions similar to (29)–(33), which determine the impedance of a metal place for "plus" polarization, it is necessary to replace q_1 in (29) and (31) by the corresponding root q_1^+ of the dispersion equation $D_+(q) = 0$, and replace α and δ by α_+ and δ_+ , where

$$\alpha_+ = (1-p) + (1+p)q_1^+ t^{-1}, \quad (34)$$

$$\delta_+ = \frac{1}{2\pi i} \int_{c_+} \frac{q dq}{D_+(q)} \frac{e^{iqL}}{1 + pe^{iqL}}, \quad (35)$$

the contour C_+ encircles counterclockwise the cut drawn from the point $1 + i\gamma$ to ∞ . It is easy to show in the general case that at $\xi \ll 1$ the second term of (29) is independent of the polarization and is proportional to ξ , while δ_+ coincides with the second term of (32) (the asterisk denotes the complex conjugate). In addition, q_1^* and q_1 are equal for a compensated metal in a strong fields, therefore also $Z_p^+ = Z_p$.

Finally, to obtain general expressions for the impedance of a symmetrically excited plate it is necessary to replace t_1^{-1} by t_1 in (29), (30), and (34), and reverse the common sign and the sign of p in the denominators of expressions (32) and (35) for δ_{\pm} . When these replacements are made, expressions (28) and (33) for the impedance remain valid.

§2. WAVEFORM OF IMPEDANCE OSCILLATIONS

The specularity coefficient is usually not too close to unity, and it can be assumed that the inequality $|q_1| \ll 1 - p$ is valid. This simplifies noticeably the expression for the impedance, which takes the form

$$Z = Z_p \left[1 - \frac{aZ_p(1-p)^2\delta}{1 + aZ_p(1-p)^2\delta} \right], \quad (36)$$

$$(aZ_p)^{-1} = q_1 \frac{1 + e^{iq_1 L}}{1 - e^{iq_1 L}} + \frac{1-p}{2\pi i} \int_c \frac{q^2 dq}{D(q)}. \quad (37)$$

The contribution of the doppleron pole was neglected in (37). For the parabolic-lens model it is important and equals $(1-p)\xi/2$. It is just Eqs. (36), (37), and (32), (35) which we shall analyze below for the case of antisymmetric excitation. These equations were deduced in Ref. 9 from simple physical considerations.

1. If a field region exists where the first term of (32) greatly exceeds the second, the rapidly oscillating part of the impedance takes in this region the quite simple form

$$\Delta Z \equiv \Delta R - i\Delta X = (1-p)^2 aZ_p^2 b_0 e^{-q_2'' L} \frac{\exp(iq_2' L)}{1 + \lambda \exp(iq_2' L)}, \quad (38)$$

where

$$\lambda = p \exp(-q_2'' L) - aZ_p(1-p)^2 b_0 \exp(-q_2'' L), \quad (39)$$

and $q_2' = \text{Re } q_2$ and $q_2'' = \text{Im } q_2$ are the real and imaginary part of the dimensionless doppleron wave vector. It follows from (38) that the oscillations of the surface resistance $R = \text{Re } Z$ and of the reactance $X = -\text{Im } Z$ are not sinusoidal and their distortion is characterized by the parameter $\eta = |\lambda|$. The distortion is due to two factors. The less interesting waveform distortion is due to the fact that even in the case of short-wave reflection of the electrons the short-wave components are multiply reflected. The influence of this factor depends essentially on the magnetic field strength. More interesting is the distortion due to multiple reflections of the short-wave components and caused by specularly reflected electrons.

The total swing of the oscillations in one period is

$$2r = \max \Delta R - \min \Delta R = \max \Delta X - \min \Delta X \quad (40)$$

and is also expressed in terms of the parameter η :

$$2r = a(1-p)^2 \exp(-q_2''L) |Z_p^2 b_0| \frac{2}{(1-\eta^2)}. \quad (41)$$

We can therefore obtain from (39) and (41), recognizing that $b_0 < 0$, the value

$$p \exp(-q_2''L) = \left\{ \eta^2 - \left[\frac{rX_p}{R_p^2 + X_p^2} (1-\eta^2) \right]^2 \right\}^{1/2} - \frac{rR_p}{R_p^2 + X_p^2} (1-\eta^2), \quad (42)$$

where $R_p = \text{Re } Z_p$, $X_p = -\text{Im } Z_p$. At $\xi \ll 1$ we have $q_2''L \rightarrow d/l$ ($l = u/2\pi\gamma$).

We emphasize that to determine $p \exp(-q_2''L)$ we need only experimental plots of R and X (and possibly of their derivatives), but there is no need whatever to know the singularities of the nonlocal conductivity of the metal. To determine the dopplerson damping length q_2'' we need plots of the oscillations for two samples of unequal thickness but cut from the same ingot and having equal surface quality. As a result we can determine the specularity coefficient p . Among the advantages of this method should be also the fact that it is contactless as well as that it can be used to determine quite small values of p .

2. We have assumed above that the specularity coefficient p is the same for all the electrons. Let us see how (29)–(33) change when the coefficient p depends on the longitudinal electron velocity. The short-wave components in strong fields ($\xi \ll 1$; $L \gg 1$), are due to resonant electrons with large longitudinal velocity. Therefore in (30)–(33) the parameter p , which is not contained in Z_p , pertains to resonant electrons.

The second term in Eq. (29) or (37) for the smooth part of the impedance is determined by all the electrons. Therefore the quantity p in these formulas has the meaning of a certain mean value. In addition, to calculate Z_p it is necessary to know the shape of the entire Fermi surface. It is for these two reasons that we have strived to express the specularity coefficient p for the resonant electrons in terms of the experimental values of the smooth part of the impedance [see (42)].

Finally, a remark concerning uncompensated metals in which helicons are present. It follows from (37) that if q_1 is the wave vector of a helicon, the waveform of the helicon oscillations also depends on the specularity coefficient. For the reasons indicated above, however, it is impossible to determine from these oscillations the value of p that pertains to any definite electrons.

3. In the “plus” polarization there are no dopplerson oscillations. In the “minus” polarization in the strongest fields, the dopplerson oscillations can be neglected and only the Gantmakher-Kaner oscillations remain. For these oscillations, which are due to the function δ_+ (35) [or to the second terms in (32)], it is impossible to write down a simple formula similar to (38). We therefore expand the rapidly oscillating part of the impedance in each period in a Fourier series and retain only the first two terms:

$$Z = Z_p \{ 1 - aZ_p(1-p)^2 e_{\text{GK}}(L) + aZ_p(1-p)^2 \times [aZ_p(1-p)^2 e_{\text{GK}}^2(L) + p e_{\text{GK}}(2L)] + \dots \}, \quad (43)$$

where we have introduced the notation

$$e_{\text{GK}}(L) = \pm \frac{1}{2\pi i} \int_{c_{\pm}} \frac{q e^{iqL}}{D_{\pm}(q)} dq. \quad (44)$$

Further analysis calls for knowledge of the conductivity singularities. It was shown in Ref. 10 that in a geometry where the [100] axis is parallel to the magnetic field and to the normal to the plate surface, tungsten is sufficiently well described with the aid of a corrugated-Fermi-surface model. We shall discuss this model in greater detail.

The function (44) was calculated in this model in Ref. 11. It can be represented, if the inequalities $\xi \ll 1$ and $L \gg 1$ are satisfied, in the form

$$e_{\text{GK}}(L) = \frac{\xi}{(2\pi L)^{1/2}} \varphi_{\pm}(x) \exp \left[-\frac{d}{l} \pm i \left(L + \frac{\pi}{4} \right) \right], \quad (45)$$

where

$$\varphi_{\pm}(x) = \frac{1}{\pi^{1/2}} \int_0^{\infty} \frac{t^{1/2}}{t \mp ix} e^{-t} dt, \quad x = \frac{L\xi^2}{2}, \quad (46)$$

and $l = u/2\pi\gamma$ is the mean free path of the resonant electrons. We calculate now the modulus of the amplitude ratio of the second and first harmonics

$$\eta = \left| p e^{-d/l} \left| \frac{\varphi(2x)}{2^{1/2}\varphi(x)} \right| + |aZ_p(1-p)^2 e_{\text{GK}}(L)| \times \exp \left\{ i \left[\arg(aZ_p) \pm \left(2 \arg \varphi_+(x) - \arg \varphi_+(2x) + \frac{\pi}{4} \right) \right] \right\} \right|. \quad (47)$$

The quantities η and $\arg(aZ_p) = -\arctan(X_p/R_p)$ are obtained from experiment. Plots of the functions $M(x)$ and $\Phi(x)$

$$M(x) = |\varphi(2x)/2^{1/2}\varphi(x)|, \\ \Phi(x) = 2 \arg \varphi_+(x) - \arg \varphi_+(2x) + \pi/4,$$

are shown in Fig. 1. Finally, the quantity $|aZ_p(1-p)^2 e_{\text{GK}}(L)|$ is equal to the ratio of the first-harmonic amplitude to $(R_p^2 = X_p^2)^{1/2}$. Thus, relation (47) makes it possible to calculate $p \exp(-d/l)$ and, in final analysis, the specularity coefficient p .

4. In the case of linear polarization and symmetric excitation, we can go to the limit as $\omega \rightarrow 0$. This situation corresponds to measurement of the transverse magnetoresistance and of the Sondheimer oscillations. The plate resistivity ρ is connected with the impedances Z_{\pm}^s by the relation

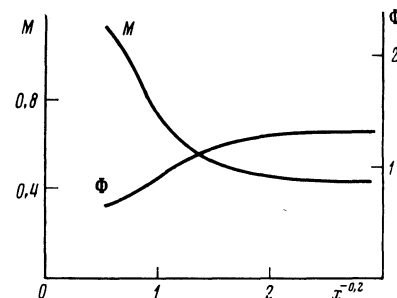


FIG. 1.

$$\frac{1}{\rho} = \frac{2}{d} \lim_{\omega \rightarrow 0} \operatorname{Re} \left(\frac{1}{Z_+^s} + \frac{1}{Z_-^s} \right), \quad (48)$$

where the superscript s labels quantities pertaining to symmetric excitation. Using expressions analogous to (28)–(32), (34), and (35) and carrying out identity transformations, we obtain

$$\frac{1}{\rho} = \frac{1}{\rho_0} \left[1 + \rho_0 \frac{c(1-p)^2}{2\pi d} \lim_{\omega \rightarrow 0} \left(\frac{1}{q_0} \operatorname{Re} \delta^s \right) \right], \quad (49)$$

where ρ_0 is the smooth part of the plate magnetoresistance. The second term in (49) describes Sondheimer oscillations. They have not only a fundamental but also multiple harmonics. To find the ratio g of the amplitude of the second harmonic of $1/\rho$ to the first, it suffices to know, as can be seen from the definition (35) of δ , the dependence, on the thickness d , of the function

$$F(d) = \lim_{\omega \rightarrow 0} \frac{1}{\omega} |e_{\text{GK}}(d)| e^{d/l}. \quad (50)$$

If the Fermi surface is such that the largest displacement is experienced by the electrons of the elliptic limiting point, then $F \propto d^{-2}$ and $g = (p/4) \exp(-d/l)$ (Ref. 12). For a parabolic limiting point, $F(d) \propto d^{-1}$ and g is twice as large. For the corrugated-cylinder model, $F(d) \propto d^{-1/2}$ and this ratio turns out to be $(p/2^{1/2}) \exp(-d/l)$. A special case is that of a parabolic lens, for which $e_{\text{GK}} = 0$ and the function $\omega^{-1} \delta^s$ is determined by the first term of (32). In this case $g = p \exp(-d/l)$.

It is customary to measure in the experiment ρ rather than $1/\rho$. For the corrugated-cylinder model the ratio of the amplitude ρ_2 of the second harmonic to that of the first ρ_1 is given by the expression

$$\left[\left(\frac{p}{2^{1/2}} e^{-d/l} + \frac{\rho_1}{8^{1/2} \rho_0} \right)^2 + \frac{\rho_1^2}{8\rho_0^2} \right]^{1/2}, \quad (51)$$

and the ratio ρ_1/ρ_0 is proportional to $L^{-1/2}$. The first term in the round brackets corresponds to the result of Ref. 2, and the corrections were written by us because they can be appreciable at small p and at not too large L . For elliptical and parabolic limiting points corrections of this kind are immaterial, for in these cases the ratio ρ_1/ρ_0 is proportional to L^{-2} and L^{-1} , respectively. For the parabolic-lens model the ratio ρ_1/ρ_0 does not contain the small parameter $1/L$ and the ratio ρ_2/ρ_1 must be calculated accurately:

$$\begin{aligned} \frac{\rho_2}{\rho_1} &= -\frac{1}{\mu} (1 - (1 - \mu^2)^{1/2}), \\ \mu &= \frac{1}{2} (1-p)^2 e^{-d/l} \left(\frac{d}{l} + \frac{1-p}{2} \right)^{-1} \\ &\times \left\{ 1 - p \left[p + \frac{(1-p)^2}{2} \left(\frac{d}{l} + \frac{1-p}{2} \right)^{-1} \right] e^{-2d/l} \right\}^{-1}. \end{aligned} \quad (52)$$

§3. MEASUREMENT TECHNIQUE AND REDUCTION OF RESULTS

We investigated in the experiment the impedance of tungsten and cadmium plates as a function of the constant magnetic field produced by an electromagnet or by a super-

conducting solenoid. The tungsten plates were 0.58, 1.3, and 2.89 mm thick and were cut from a single-crystal ingot with resistivity ratio $\rho_{300\text{ K}}/\rho_{4.2\text{ K}} \approx 50\,000$. One sample, 0.43 mm thick, was cut from an ingot having a resistivity ratio 35 000. The plate surfaces were mechanically ground and chemically polished. These tungsten samples were used earlier in Ref. 10. The cadmium samples, 0.4 and 1.86 mm thick, were cut by the electric-spark method from a single-crystal stock piece with a resistivity ratio 50 000 and were chemically polished. The normal to the plane coincided within 1° with the directions of the [100] and [0001] axes of tungsten and cadmium, respectively.

In most experiments the magnetic field was directed along the [100] axis for tungsten and along [0001] for cadmium. The magnetic-field orientation was established by the symmetry of the angular dependence of the period and amplitude of the oscillations, accurate to $10'$. In tungsten we investigated impedance oscillations due to the Doppler-shifted cyclotron resonance (DSCR) of the octahedron holes,¹³ and in cadmium the oscillations of the electron doppleron.¹⁴ The measurements were carried out with an autodyne and a bridge¹⁵ in the frequency interval 0.2–1.0 MHz at temperatures 1.3–4.2 K.

In the experiments we recorded the real and imaginary parts of the plate impedance in a circularly polarized rf field. The criterion of the accuracy of the polarization setting was the ratio of the oscillation amplitudes in the two circular polarizations near the doppleron threshold field, as well as the smoothness and monotonicity of the GKO envelope (in the case of tungsten) in magnetic field below the field H_m at which $R_p(H)$ reaches a maximum. The accuracy in the setting of the circular polarization did not exceed 2–3%.

2. The main purpose of the experiment was to determine the degree the impedance-oscillations anharmonicity, which is characterized by the parameter η , and to calculate subsequently the specularity coefficient p .

In the case when the impedance oscillations are due to a doppleron, the value of η can be determined by using the construction of Fig. 2, which shows a fragment of the $R(H)$ plot for tungsten. The envelopes touch the oscillation curve at the points G, H , and K . The points A, B, C, D, E , and F have the following properties: $AB = BC$, $CD = DE$, and $BD = DF$. We introduce the notation

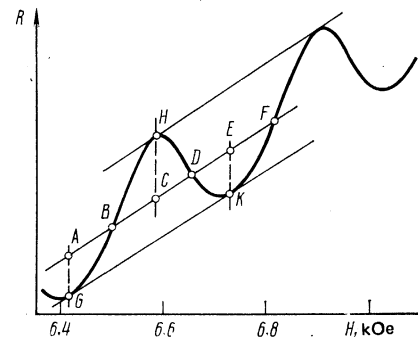


FIG. 2. Plot of $R(H)$ for tungsten sample 0.58 mm thick at $T = 4.2\text{ K}$ and $\omega/2\pi = 490\text{ kHz}$. Calculation using Eqs. (53) and (54) yields $\eta_D = 0.13$.

$$y = 1 + 2 \left[1 - \left(\frac{\alpha - \beta}{\alpha + \beta} \right)^2 \right] \left[\left(\frac{\alpha - \beta}{\alpha + \beta} \right)^2 + \text{ctg}^2 \psi \right]^{-1}, \quad (53)$$

It can be shown that η is connected with y by the relation

$$\eta = [y - (y^2 - 1)^{1/2}]^{1/2}. \quad (54)$$

At small η this method has low accuracy. In addition, it cannot be used to analyze the anharmonicity of the GKO. In those cases we expanded the experimentally obtained function ΔR (or ΔX) in a Fourier series over one period, since in all cases the ratio second and first harmonics is equal to η . In practice it is much more convenient and accurate to do this by using the plots of the first or second derivative of the surface resistance (or reactance) with respect to the magnetic field. To record the derivatives of R and X we used a modulation technique. At low modulation amplitude h ($h \ll \Delta H$, where ΔH is the period of the oscillations) the recorded signals at the modulation frequency and at double this frequency are proportional respectively to the derivatives dZ/dH and d^2Z/dH^2 . Expanding the derivatives in Fourier series, we find the ratio of the amplitudes of the second and first derivative. This ratio is equal to 2η for dZ/dH and 4η for d^2Z/dH^2 .

The impedance oscillations are not quite periodic: their amplitude, and in the case of the doppleron also the period, depends on the magnetic field. We have therefore introduced corrections to allow for the changes of these parameters. In all cases the correction to η , due to the nonperiodicity, did not exceed 10%.

3. The modulation technique offers many more possibilities than merely of recording the derivatives of R and Y . By choosing the modulation amplitude it is possible to suppress oscillations of a definite period ΔH_0 . Indeed, for a harmonic function $V(H) = V_0 \cos(2\pi H / \Delta H)$ the signal V_1 recorded at the modulation frequency has an amplitude $V_0 J_1(x)$, and V_2 at double the frequency has an amplitude

$$V_0 J_2(x), \quad (55)$$

where J_k is a Bessel function and $x = 2\pi h / \Delta H$. Choosing h such that x for $\Delta H = \Delta H_0$ coincides with the zero x_0 of the corresponding Bessel function, we cause the recorded signal

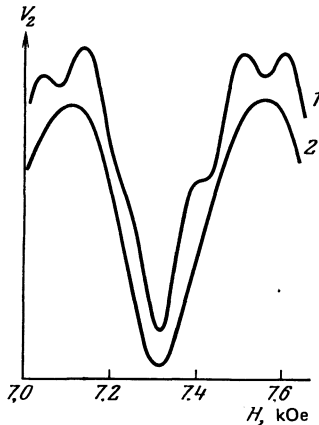


FIG. 3. Plots of oscillations in minus polarization for a tungsten plate with $d = 0.43$ mm at $T = 4.2$ K, $\omega/2\pi = 260$ kHz.

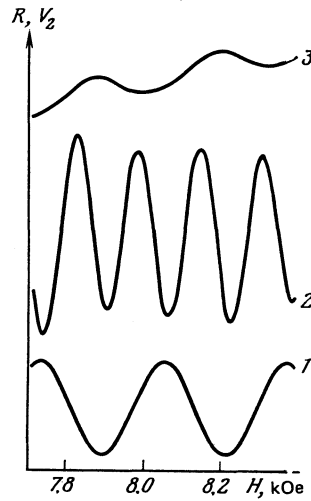


FIG. 4. Oscillations in a tungsten plate with $d = 0.58$ mm in plus polarization; $T = 4.2$ K, $\omega/2\pi = 490$ kHz. Curves 1 and 2 were obtained by the modulation method. Curve 3—plot of $R(H)$ in arbitrary unit, $R(H)$ reckoned from the abscissa axis.

of the given period to vanish. We used this procedure for two purposes.

First, to suppress the impedance oscillations due to DSCR of another group of carriers. This is illustrated in Fig. 3, which shows plots of the signal at double the modulation frequency for a tungsten plate at two values of h . Curve 1 correspond to small h and represents in fact the derivative d^2R_-/dH^2 . It reveals, besides the oscillations due to the DSCR of the octahedron hole, also oscillations with a period smaller by a factor 3.8. These oscillations have a noticeable amplitude in the field region $H \sim 2H_L$. Curve 2 corresponds to the value of h at which there are no oscillations with the smaller period. In this case the amplitude ratio of the second and first harmonics, obtained from curve 2, is not equal to 4η . In accord with (55), to calculate η the ratio of the harmonics must be multiplied by $J_2(x)/J_2(2x)$, where $x = x_0/3.8$.

Second, the determination of the parameter η can be greatly simplified in the case when the oscillations of Z are due to one carrier group, and their period and amplitude depend little on the magnetic field. By choosing the value of h we can suppress the first harmonic. The registered signal is due in this case predominantly to the second harmonic. The parameter η is determined by the ratio

$$\eta = \frac{A_2 J_2(x_0/2)}{A_1 J_2(2x_0)}, \quad (56)$$

where A_2 is the amplitude of the second harmonic from the first plot, and A_1 the amplitude of the first harmonic from the second plot. The measurements were made mainly at double the modulation frequency, for in this case there is practically no monotonic variation of the signal with the magnetic field. The use of the described method is illustrated in Fig. 4. It shows plots of the Doppler oscillations in tungsten in fields in which the oscillation amplitude is a maximum and the GKO amplitude is small. Curve 1 represents mainly the first harmonic, and curve 2 the second. Curve 2 is

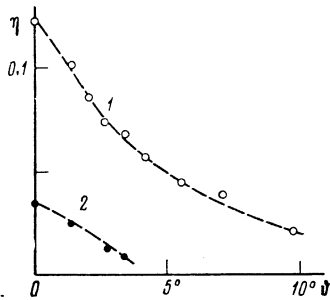


FIG. 5. Plot of $\eta(\vartheta)$ for tungsten sample 0.58 mm thick, obtained from measurements at $T = 4.2$ K, $\omega/2\pi = 490$ kHz.

obtained at a gain 30 times larger than curve 1.

The described method makes it possible to determine simply and reliably the parameter η . Its effective use calls for high monochromaticity and stability of the modulation field. In our experiments the coefficients of the harmonics and the instability of this field did not exceed 10^{-4} .

§4. MEASUREMENT RESULTS

For each of the investigated tungsten samples, the values of η determined by different methods were close. Table I lists the value of η obtained from the doppleron oscillations (η_D) and from the GKO (η_{GKO}), for samples having different thicknesses and different electron mean free paths. The values of η_D were obtained from plots in the field interval $1.9 < H/H_L < 2.5$, in which the contribution of the GKO to Z_+ could be neglected.

The oscillation anharmonicity decreases markedly when the magnetic field is inclined away from the [100] axis. The dependence of η on the angle ϑ is shown in Fig. 5. The light circles, which pertain to doppleron oscillations, were obtained in the field interval $(2.3-2.5)H_L$. The dark circles were obtained for the GKO in fields $(5-5.3)H_L$.

For cadmium we investigated the doppleron oscillations due to DSCR of the lentil electrons at $H \parallel [0001]$. The Gantmakher-Kanner oscillations due to the same group of carriers have a much smaller amplitude.¹¹ In contrast to the situation in tungsten, the amplitude and period of the dop-



FIG. 6. Oscillations of electron doppleron d^2R/dH^2 in a cadmium plate; $d = 0.4$ mm, $T = 1.6$ K, $\omega/2\pi = 260$ kHz.

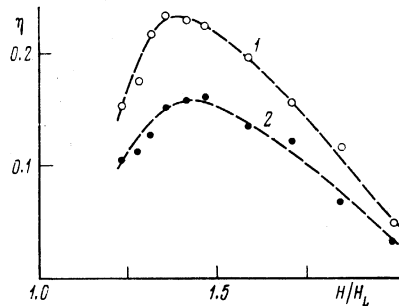


FIG. 7. Anharmonicity parameter of doppleron oscillations in cadmium vs. the magnetic field. Curve 1—measurements for a plate with $d = 1.86$ mm at $T = 1.6$ K, $\omega/2\pi = 300$ kHz; curve 2—reduction of results in accord with Eqs. (59) and (60).

pleron oscillations in cadmium depend strongly on the magnetic field. Under these conditions, the method of suppressing the first harmonic is not very effective. The value of η was therefore determined by Fourier analysis of the plots of dR/dH and d^2R/dH^2 . A striking example of the oscillation anharmonicity in cadmium is shown in Fig. 6. The measurements of η were performed in magnetic fields $H < 2H_L$, inasmuch as in stronger fields the oscillation amplitude and the value of η decrease rapidly and the accuracy of η is decreased. The dependence of η on H is shown in Fig. 7 (curve 1).

To determine $p \exp(-dl)$ from (42) and (47) we need, besides η , the values of the smooth parts of the surface resistance R_p and of the reactance X_p , and also the total swing r of the oscillations. We therefore measured, besides the plots obtained by the modulation technique, the plots of $R(H)$ and $X(H)$. A fragment of the $R(H)$ plot is shown in Fig. 4 (curve 3).

5. DISCUSSION

1. Equations (42) and (47) contain the mean free path l of the resonant carriers. According to Ref. 10, the value of l in tungsten samples with resistivity ratio 50 000 is close to 1 mm at $T = 4.2$ K. For the sample with the resistivity ratio 35 000 we assumed $l = 0.7$ mm. The values of p calculated from the doppleron oscillations are given in the fourth column of Table I, and those obtained from the GKO in fifth column. (The result for the sample with $d = 0.43$ mm were published earlier.⁹) Since the plates were produced by the same technology, it is natural to expect for them close values of p . The fact that the obtained values of p did indeed turn out to be close justifies the choice of l (a change of l by only 20% leads to a large scatter of the values of p).

The determination of p from the GKO in a wide range of magnetic fields reveals that p has a tendency to decrease with increasing H . In the fifth column of Table I are shown

TABLE I.

d , mm	η_D	η_{GKO}	p_D	p_{GKO}
	2	3	4	5
0.43	0.14	0.045	0.16	0.15
0.58	0.12	0.031	0.13	0.10
1.30	0.065	—	0.15	—
2.89	0.015	—	0.15	—

the values of p obtained in the field range where the GKO are maximal. Since this region corresponds to fields stronger than those at which the doppleron oscillations are maximal, the values of p in the fifth columns are somewhat smaller than in the fourth. The parameter η for the KGO is smaller than for doppleron oscillations. In addition the GKO in thick samples have small amplitudes. We have therefore not attempted to determine the specularly coefficient of thick samples from the GKO. We emphasize finally once more that to determine p from the GKO we must know the singularities of the nonlocal conductivity.

2. It can be seen from Fig. 5 that the anharmonicities of doppleron oscillations and of the GKO decrease when the magnetic field is inclined. The reason is that in the case of specular reflection in an inclined field the carrier longitudinal velocity changes. Therefore some of the specularly reflected electrons cease to be resonant. As a result, the effective specularly coefficient decreases. The behavior of the curves of Fig. 5 is direct experimental proof of this effect. We note that the possibility that p depends on the field inclination angle was discussed in an elucidation¹⁶ of the nature of the impedance oscillations of zinc. It was noted earlier¹² that the amplitudes of the multiple harmonics in the Sondheimer effect should also decrease when the vector \mathbf{H} is inclined away from the normal to the surface.

3. The experiments with cadmium illustrate the difficulty of applying to the proposed method of determining p . The point is that the doppleron oscillations are observed in cadmium in the field region where the inequality $\xi \ll 1$ is not satisfied. The theory developed above is strictly speaking not applicable in this case. We shall nonetheless attempt to obtain some estimates. A theory of the impedance of a plate with diffusely reflecting surfaces in weak fields was developed in Ref. 3. In the case when the GKO can be neglected, we can obtain from Eqs. (44), (45), (52), (53), and (55) of Ref. 3 an expression similar to (38) for the oscillating part of the impedance:

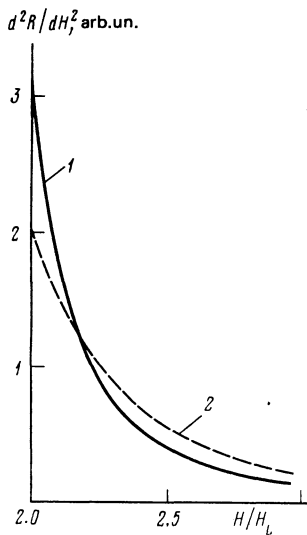


FIG. 8. Calculated envelopes of the derivative d^2R/dH^2 of doppleron oscillations. Curve 1) $p = 0$, 2) $p = 0.5$.

$$\Delta Z_0 = -Z_0 \frac{A e^{i q_2' L}}{1 + \lambda_0 e^{i q_2' L}}, \quad (57)$$

where

$$A = a b_0^2 D'(q_2) Z_0 e^{-q_2' L}, \quad \lambda_0 = A I, \\ I = 1 + i e_0'(0) / 2 q_2, \quad (58)$$

Z_0 is the value of Z_p at $p = 0$, and b_0 is determined now by Eqs. (10) and (7) of Ref. 3. Expressions (57) and (58) are valid at $|q_1| \ll |q_2|$, $L \gg 1$. These equations enable us to express the anharmonicity parameter η_0 in terms of the total swing r of the oscillations, the smooth part of the impedance Z_0 , and the value of I :

$$\eta_0 = \left(1 + \frac{1}{4 r^2} \left| \frac{Z_0}{I} \right|^2 \right)^{1/2} - \frac{1}{2 r} \left| \frac{Z_0}{I} \right|. \quad (59)$$

The quantity I is expressed in terms of the doppleron wave vector k_2 and the impedance of a sufficiently thick plate (such that the maximum of $R_p(h)$ occurs in a field much stronger than that of interest to us):

$$I = 1 - \frac{1}{k_2(H) d} \frac{X(H \rightarrow \infty)}{Z(H)}. \quad (60)$$

If we assume now that purely diffuse reflection takes place in the experiment, we can substitute the experimental values of r , Z_0 , and I in (59) and calculate the expected value of η_0 (I was determined for a sample 1.86 mm thick). The result of such a calculation is represented by curve 2 of Fig. 7. This curve is similar to curve 1, but lies somewhat lower. It is natural to assume that this difference is due to the fact that p is finite. As a result we get the estimate $p \exp(-d/l) \approx 0.05$. An estimate of l from the resistivity ratio yields $l \approx 2$ mm. It follows therefore that the order of magnitude of p is 0.1 to 0.2. For a quantitative determination of p it is necessary to develop a theory that is valid in the region of moderate fields $\xi \sim 1$ and at an arbitrary value of p .

4. We note in conclusion that although the oscillation amplitude of the impedance Z as a function of p has a maximum at $p = 0$, this may not be the case for the derivatives of the impedance with respect to the magnetic field. The presence of multiple harmonics makes the oscillations sharper and therefore the maximum amplitude of the d^2Z/dH^2 oscillations as functions of p may be reached at $p \neq 0$. This is illustrated in Fig. 8, which shows the calculation results for a sample 0.15 mm thick. In the field region $H < 2.2 H_L$ the amplitude of the d^2R/dH^2 oscillations is larger at $p = 0$ than at $p = 0.5$. At the same time, in the region $H > 2.2 H_L$ the amplitude ratio is inverted. Therefore a comparison of the amplitude of the d^2Z/dH^2 oscillations at different samples surface states does not permit an unequivocal assessment of the relation between the corresponding value of p .

¹V. S. Tsoi, Zh. Eksp. Teor. Fiz. **68**, 1849 (1975) [Sov. Phys. JETP **41**, 927 (1975)].

²A. M. Grishin, P. P. Lutsishin, Yu. S. Ostroukhov, and O. A. Panchenko, Zh. Eksp. Teor. Fiz. **76**, 1325 (1979) [Sov. Phys. JETP **49**, 673 (1979)].

³I. F. Voloshin, V. G. Skobov, L. M. Fisher, and A. S. Chernov, Zh. Eksp. Teor. Fiz. **80**, 183 (1981) [Sov. Phys. JETP **53**, 92 (1981)].

⁴G. E. H. Reuter and E. H. Sondheimer, Proc. Roy. Soc. **A176**, 336 (1948).

- ⁵P. M. Platzman and S. J. Buchsbaum, *Phys. Rev.* **132**, 2 (1963).
- ⁶D. E. Zherebchevskii and V. P. Naberezhnykh, *Fiz. Nizk. Temp.* **4**, 467 (1978) [*Sov. J. Low Temp. Phys.* **4**, 229 (1978)].
- ⁷I. F. Voloshin, S. V. Medvedev, V. G. Skobov, L. M. Fisher, and A. S. Chernov, *Zh. Eksp. Teor. Fiz.* **71**, 1555 (1976) [*Sov. Phys. JETP* **44**, 814 (1976)].
- ⁸D. Falk, B. Gerson, and L. Carolane, *Phys. Rev.* **B1**, 404 (1970).
- ⁹I. F. Voloshin, N. A. Bodlevskikh, V. G. Skobov, L. M. Fisher, and A. S. Chernov, *Pis'ma Zh. Eksp. Teor. Fiz.* **35**, 238 (1982) [*JETP Lett.* **35**, 235 (1982)].
- ¹⁰I. F. Voloshin, V. G. Skobov, L. M. Fisher, and A. S. Chernov, *Zh. Eksp. Teor. Fiz.* **82**, 293 (1982) [*Sov. Phys. JETP* **55**, 175 (1982)].
- ¹¹I. F. Voloshin, V. G. Skobov, L. M. Fisher, and A. S. Chernov, *Zh. Eksp. Teor. Fiz.* **72**, 735 (1977) [*Sov. Phys. JETP* **45**, 385 (1977)].
- ¹²Yu. M. Goland, *Fiz. Tverd. Tela (Leningrad)* **10**, 81 (1968). [*Sov. Phys. Solid State* **10**, 58 (1968)].
- ¹³I. M. Vitebskii, V. V. Vitchinkin, A. A. Galkin, Yu. A. Ostroukov, O. A. Panchenko, L. T. Tsymbal, and A. N. Cherkasov, *Fiz. Nizk. Temp.* **1**, 400 (1975) [*Sov. J. Low Temp. Phys.* **1**, 200 (1975)].
- ¹⁴L. M. Fisher, V. V. Lavrova, V. A. Yudin, O. V. Konstantinov, *Zh. Eksp. Teor. Fiz.* **66**, 759 (1971) [*Sov. Phys. JETP* **33**, 410 (1971)].
- ¹⁵I. F. Voloshin, V. G. Skobov, L. M. Fisher, A. S. Chernov, and V. A. Yudin, *Zh. Eksp. Teor. Fiz.* **73**, 1884 (1977) [*Sov. Phys. JETP* **46**, 989 (1977)].
- ¹⁶A. A. Galkin, V. A. Mishin, L. T. Tsymbal, and A. N. Cherkasov, *Zh. Eksp. Teor. Fiz.* **80**, 1981 (1981) [*Sov. Phys. JETP* **53**, 1030 (1980)].

Translated by J. G. Adashko